

170 (1967).

⁷V. Bargmann, *Z. Physik* **99**, 576 (1936).⁸L. C. Biedenharn, *J. Math. Phys.* **2**, 433 (1961).⁹L. Infeld and T. E. Hull, *Rev. Mod. Phys.* **23**, 21 (1951).¹⁰G. Feinberg, *Phys. Rev.* **112**, 1637 (1958).¹¹S. Pasternack and R. M. Sternheimer, *J. Math.**Phys.* **3**, 1280 (1962).¹²Additional discussion of this point will be given elsewhere.¹³S. Feneuille, *Compt. Rend.* **B271**, 992 (1970).¹⁴A discussion of the R_{nl} is given in H. A. Bethe and E. E. Salpeter, *Quantum Mechanics of One- and Two-Electron Atoms* (Academic, New York, 1957).

PHYSICAL REVIEW A

VOLUME 5, NUMBER 6

JUNE 1972

Origin of the Silver L -Series X-Ray Spectrum*

E. J. McGuire

Sandia Laboratories, Albuquerque, New Mexico 87115

(Received 15 December 1971)

Using recently calculated values of radiative, Coster-Kronig, and Auger transition rates, and the hypothesis that the satellite structure arises from doubly ionized atoms (with L and N holes), and an assumed incident x-ray spectrum, we calculate the relative intensities of the Ag L -series x-ray spectrum. The calculations are in best agreement with Parratt's measurements when Ag L_1 - $L_3M_{4,5}$ Coster-Kronig transitions are forbidden. Comparison of the calculations with the satellite components leads to unsatisfactory agreement. Reasons for this are discussed. Modified values of f_{12} , f_{13} , and ω_1 for the Ag and Sn L shells are reported.

I. INTRODUCTION

In a 1937 review article on x-ray satellite structure,¹ Richtmyer pointed out that while a multiple-ionization theory² could adequately account for the $K\alpha$ satellite spectrum it was unable to predict the peculiar phenomena associated with L -shell satellite spectra. To account for the latter, Richtmyer argued that Auger processes were necessary. However, it is only recently³⁻⁷ that reliable calculated Auger transition rates have become available. In the future, we plan an extensive comparison of calculated and experimental satellite structure but for the present we confine our examination to silver. Parratt⁸ has made a precision measurement of the Ag L -series x-ray spectrum. As an indication of the sensitivity involved, Parratt measured the intensity of the L_2 - N_1 line as 0.28 compared to the L_3 - M_5 line with intensity 100. As we shall see, the calculation leads to 0.30 for the intensity of L_2 - N_1 when L_3 - M_5 is set equal to 100. The motivation for this study arose neither from the diagram line intensities nor from the satellite structure but rather from the value of the width (lifetime) of an L_1 hole. Parratt measured an average width for the L_1 - $M_{2,3}$ transition as 6.25 eV, while for the much weaker L_1 - $M_{4,5}$ transition (a nondipole transition) he found a width of 5.8 eV. The author has recently calculated the $M_{4,5}$ and $M_{2,3}$ widths as 0.44 and 3.80 eV.³ Thus, from the measured L_1 - $M_{2,3}$ width one deduces 2.45 eV as the width due to the lifetime of the L_1 hole; yet from the L_1 - $M_{4,5}$ width one deduces an L_1 width of 5.4 eV. In addition, the author has

calculated⁴ an L_1 width of 9.03 eV while Crasemann *et al.*⁶ obtain 7.56 eV. The calculated values are so large because it is assumed L_1 - $L_3M_{4,5}$ Coster-Kronig transitions are energetically allowed. An inaccurate way of estimating the continuum electron energy in an nl - $n'l'n''l''$ Auger transition is to use

$$\epsilon_1(Z) = -E_{nl}(Z) + E_{n'l'}(Z) + E_{n''l''}(Z), \quad (1)$$

where E_{nl} is a one-electron ionization threshold and ϵ_1 is the estimated energy of the continuum Auger electron. Three more accurate procedures are

$$\epsilon_2(Z) = -E_{nl}(Z) + E_{n'l'}(Z) + E_{n''l''}(Z+1), \quad (2)$$

$$\epsilon_3(Z) = -E_{nl}(Z) + E_{n'l'}(Z+1) + E_{n''l''}(Z), \quad (3)$$

$$\epsilon_4(Z) = -E_{nl}(Z) + \frac{1}{2}[E_{n'l'}(Z) + E_{n''l''}(Z+1) + E_{n''l''}(Z) + E_{n'l'}(Z+1)] \quad (4)$$

For instance, estimate (1) would allow a large L_1 - L_3M_5 Coster-Kronig transition rate at $Z=73$. The other estimates indicate such a transition is energetically forbidden. Experimental measurements on $f_{1,3}$ indicate the transitions do not occur.⁴ For the silver L_1 - $L_3(M_4, M_5)$ transition estimate (2) leads to $\epsilon_2 = (+44 \text{ eV}, +51 \text{ eV})$ for the continuum electron energy, where we use the ESCA⁹ tabulation of ionization thresholds. Estimate (3) leads to $\epsilon_3 = (-105 \text{ eV}, -99 \text{ eV})$, while estimate (4) leads to $\epsilon_4 = (-31 \text{ eV}, -27 \text{ eV})$. Thus two of the estimates predict the transition is energetically forbidden, one predicts it is allowed. The point of this paper is to examine the effect of the presence or absence of

TABLE I. Four sets of parameters for $f_{1,2}$, $f_{1,3}$, and Γ_{L_1} for the L_1 shell of Ag.

Case	$f_{1,2}$	$f_{1,3}$	Γ_{L_1} (eV)
(i)	0.167	0.313	2.81
(ii)	0.074	0.692	6.31
(iii)	0.052	0.786	9.01
Ref. 6	0.064	0.695	7.56

the $L_1-L_3M_{4,5}$ transition on the L_1 width and on the relative intensities of both the diagram and satellite lines. In fact, we will also examine the possibility that the $L_1-L_3M_4$ transition is forbidden while the $L_1-L_3M_5$ transition is allowed.

II. CALCULATIONS

In Table I we list the Coster-Kronig yields and L_1 width for three cases: (i) Both $L_1-L_3M_4$ and $L_1-L_3M_5$ transitions are forbidden; (ii) the $L_1-L_3M_4$ transition is forbidden but the $L_1-L_3M_5$ transition is allowed; and (iii) both transitions are allowed. We also include the results of Crasemann *et al.*⁶ From Table I it can be seen that the L_1 width for case (i) 2.81 eV is in reasonable agreement with the value derived from the $L_1-M_{2,3}$ width, 2.45 eV. However, the width obtained for case (ii) 6.31 eV is reasonably close to the value 5.4 eV derived from the weak $L_1-M_{4,5}$ line. Thus, the comparison of the three cases with the experimental width determinations is not entirely conclusive.

Because Parratt's article⁸ is perhaps not readily available and because we introduce gross satellite definitions, we reproduce Parratt's identifications and intensities in Table II, along with the energy difference associated with the measured wavelength. The symbol S is used to indicate a satellite line and the S_i are defined in the table. We reserve the examination of the details of the satellite structure for Sec. III.

In Parratt's experiment the silver target was bombarded with an x-ray beam created by 15-keV electrons striking gold. Photoionization leads to an initial hole population of N_1L_1 holes, N_2L_2 holes, and N_3L_3 holes. We assume that the initial population decays by Coster-Kronig transitions to a final L -shell hole population before radiating (the Coster-Kronig rates in all cases are at least five times the total radiative rates). Thus, we have a population after Coster-Kronig transitions given by

$$\begin{aligned}
 N_1 &= N_1(1 - f_{12} - f_{13}), & N_2 &= N_2(1 - f_{2,3}), \\
 N_{2,1} &= N_1f_{12}(1 - f_{23}), & N_3 &= N_3, \\
 N_{3,1} &= N_1f_{13}, & N_{3,2} &= N_2f_{23}.
 \end{aligned}$$

Here, $f_{2,3}$ is taken as 0.152,⁴ and we have neglected small terms (e.g., $N_{321} = N_1f_{12}f_{23}$). The quantities $N_{2,1}$, $N_{3,1}$, and $N_{3,2}$ are populations of at least dou-

bly ionized atoms to which we attribute the satellite spectrum. For the analysis in terms of gross satellite structure we add $N_{3,1}$ and $N_{3,2}$.

In Parratt's x-ray tube electrons of 15 keV strike a gold anode producing an x-ray beam. This x-ray beam strikes the silver target and x rays emitted from the silver target are observed. However, the Au x-ray spectrum is not given, and to determine the initial Ag L -shell hole distribution we assume

TABLE II. Ag L -series x-ray line designations, identifications, energy differences, and measured intensities, from Ref. 8.

Line	Transition	ΔE (eV)	Satellite designation	Measured intensity
$\gamma_{2,3}''$	S	3815	...	0.06
$\gamma_{2,3}'$	S	3790	...	
γ_3	L_1N_3	3760		1.04
$\gamma_{2,3}$...	3758		
γ_2	L_1N_2	3755		0.66
$\gamma_{1,3}''$	S	3575	$S_1 \equiv S(L_2 - N_4)$	0.16
$\gamma_{1,3}'$	S	3562		
$\gamma_{1,3}$	S	3558		
γ_1	L_2N_4	3525		4.36
β_9	L_1M_5	3450		0.074
β_{10}	L_1M_4	3440		0.043
γ_5	L_2N_1	3437		0.13
β_2^{IV}	S	3400	$S_2 \equiv S(L_3 - N_3)$	1.78
β_2^V	S	3398		
$\beta_{2,3}''$	S	3395		
$\beta_{2,3}'$	S	3392		
$\beta_{2,3}$	S	3385		
β_2^a	S	3380		
β_2^b	S	...		
β_2	L_3N_5	3356		11.9
β_6	L_3N_1	3262		0.56
β_3	L_1M_3	3240		7.2
β_4	L_1M_2	3211		3.9
β_1^{IV}	S	3187	$S_3 \equiv S(L_2 - M_4)$	2.06
$\beta_{1,3}''$	S	3180		
$\beta_{1,3}'$	S	3173		
$\beta_{1,3}$	S	3164		
β_1	L_2M_4	3158		49.1
α_7	S	3020	$S_4 \equiv S(L_3 - M_{4,5})$	11.7
α_6	S	3012		
α_5	S	3004		
α_4	S	3002		
α_3	S	3000		
α_1	L_3M_5	2996		100
α_2	L_3M_4	2980		8.61
η	L_2M_1	2820		2.0
l	L_3M_1	2640		4.4

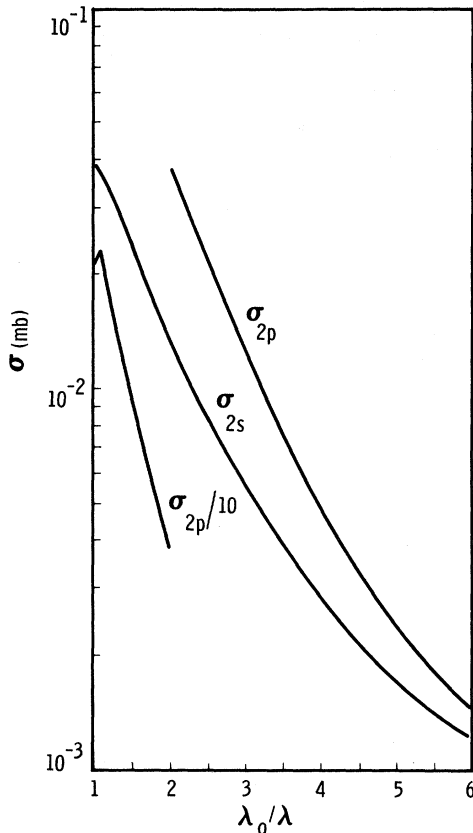


FIG. 1. Photoionization cross section for the $2s$ and $2p$ shells of Ag, where $\lambda_0 = hc/E_0$ and E_0 is the ionization threshold for the particular shell.

the x-ray output of the Au target, $N(\nu)$, has a Kramers spectrum, [i. e., $N(\nu) \propto (\nu_0 - \nu)\Theta(\nu_0 - \nu)$, where $h\nu_0 = eV_0$ and V_0 is the voltage across the x-ray tube].¹⁰ Given this shape, subshell photoionization cross sections computed by the author¹¹ shown in Fig. 1, and the ionization thresholds,⁹ we compute an approximate initial distribution $N_1/N_2/N_3 = 1.00/1.48/2.83$. With this initial hole distribution we obtain the final hole distribution shown in Table III. The column labeled (ia) is the final hole distribution following renormalization of the initial hole distribution. This is discussed below. After we have accounted for the Coster-Kronig transitions, we have two channels left, radiative and Auger transitions. The total transition rates due to the sum of these two processes (A^{\wedge}) are 539, 805, and 781 ($\times 10^{-4}/\text{a. u.}$) where 1 a. u. = 2.42×10^{-7} sec. Normalizing the radiative transition rates of Rosner and Bhalla¹² or Scofield¹³ with these modified total transition rates produces the normalized radiative transition rates listed in the second column of Table IV. Combining these with the final hole populations leads to the relative

intensities (normalized to the L_3 - M_5 diagram line) listed in columns 3, 5, and 6 in Table IV. The columns are labeled by case numbers. We do not repeat entries in Table IV unless they change. Several features stand out. The calculated intensities for the L_2 and L_3 diagram lines are in good agreement with the measurements. This indicates the calculated radiative transition rates^{12,13} are accurate. The calculated intensities for the L_1 diagram lines agree best with experiment for case (ii). However, if we examine the computed intensity for the strong satellite $S_4 = S(L_3-M_{4,5})$ we see that the calculations for case (ii) lead to a satellite intensity almost four times greater than the measurement.

However, if we argue that the assumed x-ray spectrum may be incorrect (the initial hole population is wrong) and normalize to experiment the computed intensities for transitions to the L_1 hole, we find a new initial population $N_1/N_2/N_3 = 0.607/1.48/2.83$. With this we recompute the final hole populations [the column labeled (ia) in Table III] and the relative intensities (column 4 of Table IV). The strong satellite S_4 is now in good agreement with the measurement, all the diagram lines are in good agreement with the measurements, but the weaker satellites differ from experiment by as much as a factor of 2. If we attempted the above renormalization for cases (ii) and (iii) we would be forced to increase the intensity of the satellite S_4 . Since this is already almost four times larger than the experimental value, the disagreement would be increased. Thus, we conclude that, if L_1 - $L_3M_{4,5}$ transitions are not allowed, the measured and computed line widths are in agreement to 15%, the diagram lines and the strong satellite agree to 25%, while the calculated intensity for the weaker satellites differs from experiment by as much as a factor of 2.

III. DETAILED SATELLITE STRUCTURE

We have advanced a hypothesis concerning the origin of the L satellites in silver. In addition to

TABLE III. Final hole populations after Coster-Kronig transitions but prior to radiative and Auger transitions. Cases (i), (ii), and (iii) assume an incident Kramers spectrum and no L_1 - $L_3M_{4,5}$ transition, no L_1 - L_3M_5 transition, and both L_1 - $L_3M_{4,5}$ transitions, respectively. Case (ia) is case (i) with a renormalized incident spectrum.

n case	(i)	(ia)	(ii)	(iii)
n_1	0.520	0.316	0.234	0.162
n_2	1.26	1.26	1.26	1.26
n_{21}	0.142	0.086	0.063	0.044
n_3	2.83	2.83	2.83	2.83
n_{31}	0.313	0.190	0.692	0.786
n_{32}	0.225	0.225	0.225	0.225

TABLE IV. Relative intensities for Ag L -series x-ray lines for four final hole populations and experimental values. The case designations are the same as in Table III.

Transition	Radiative rate/ A' (10^{-3})	Calculated relative intensity				Expt
		(i)	(ia)	(ii)	(iii)	
L_1M_2	18.2	6.72	4.07	3.03	2.10	3.9
M_3	30.1	11.1	6.73	5.02	3.46	7.2
M_4	0.21	0.08	0.05	0.03	0.02	0.04
M_5	0.31	0.11	0.07	0.05	0.04	0.07
N_2	3.37	1.24	0.75	0.56	0.39	0.66
N_3	5.61	2.07	1.26	0.93	0.65	1.04
L_2M_1	1.66	1.48				2.0
M_4	56.7	50.6				49.1
N_1	0.33	0.30				0.28
N_4	5.85	5.24				4.36
$S(L_2M_4)$	56.7	5.72	3.47	2.54	1.77	2.06
$S(L_3N_4)$	5.85	0.59	0.36	0.26	0.18	0.16
L_3M_1	2.06	4.14				4.4
M_4	5.61	11.3				8.61
M_5	49.8	100				100
N_1	0.40	0.80				0.56
N_5	5.02	10.1				11.9
$S(L_3M_{4,5})$	55.4	21.2	16.3	36.2	39.6	11.7
$S(L_3N_5)$	5.02	1.92	1.48	3.27	3.60	1.78

determining the intensities of the satellite groups relative to the diagram lines, Parratt⁸ has attempted a detailed analysis of the intensity of the components of the satellites. Here we compare the results of his analysis with calculations based on the hypothesized model for the satellite structure. We do not include the very weak satellite S_1 . Parratt finds five components for the satellite S_4 , four for the satellite S_3 , and six for the satellite S_2 . With our hypothesis for the origin of the satellites we would expect five components in each corresponding to an L hole and one N_i hole ($i = 1-5$). Thus, we assume the weakest line in S_3 was not resolved, while the sixth (weakest) line in S_2 is due to the analysis (it is less than 3% of the total intensity for S_2). Thus, we argue that to 5% Parratt's analysis is consistent with five component satellites. The satellite components of L_3 lines arise from both L_2-L_3N and L_1-L_3N transitions. For both sets of Coster-Kronig transitions the rates are available⁵ and coupled with the assumed initial hole distributions allow one to compute the relative populations of LN_i doubly ionized atoms. We assume that the energy shifts of the satellites from the main lines decrease with increasing i . Thus, the most strongly shifted component occurs in the ion with $L-N_1$ holes. With these assumptions, we obtain the relative intensities shown in Table V. Generally, the calculations and experiment differ in that the calculations underestimate the relative intensity of the (LN_4, N_5) satellites and overestimate the $(LN_{1,2,3})$ satellites. This could be an indication that Coster-Kronig transitions of the form $LN_1-LN_{4,5}N_{4,5}$ occur in the doubly ionized

atom, i. e., that some portion of the satellite spectrum arises from triply ionized atoms. However, this requires N -shell transition rates in the presence of an L -shell hole which are not available. Were such N -shell transitions to occur, one would not an-

TABLE V. Calculated and measured relative intensities for the components of three satellites. The notation $\alpha_7(L_3N_1)$ indicates the satellite (α_7) and the hypothesized hole distribution leading to the satellite.

Satellite	Relative intensity (calc)	Relative intensity (meas)
$\alpha_7(L_3N_1)$	0.178	0.040
$\alpha_6(L_3N_2)$	0.154	0.140
$\alpha_5(L_3N_3)$	0.179	0.266
$\alpha_4(L_3N_4)$	0.267	0.444
$\alpha_3(L_3N_5)$	0.222	0.146
$\beta_2^{IV}(L_3N_1)$	0.178	0.127
$\beta_2^V(L_3N_2)$	0.154	0.064
$\beta_{2,\dots}(L_3N_3)$	0.179	0.156
$\beta_{2,\dots}(L_3N_4)$	0.267	0.364
$\beta_{2,\dots}(L_3N_5)$	0.222	0.279
$\beta_1^{IV}(L_2N_1)$	0.269	0.049
$\beta_{1,\dots}(L_2N_2)$	0.175	0.136
$\beta_{1,\dots}(L_2N_3)$	0.282	0.407
$\beta_{1,\dots}(L_2N_{4,5})$	0.275	0.407

anticipate that the satellite would have exactly five components. However, without an accurate treatment of the energetics involved one cannot rule out such a possibility. Two alternative explanations for the difference are available. First, the calculated Coster-Kronig rates are in error and overestimate the $L_1-L_3N_1$ and $L_2-L_3N_1$ transition rates. Ideally one would like to compare the calculations with measured Coster-Kronig L_1-L_3N and L_2-L_3N electron spectra for Ag. We would expect such peaks to be in the 250–350³ eV range. However, one expects such peaks to overlap the inevitable M -shell Coster-Kronig and Auger electron spectrum. The second explanation is that the differences lie in the resolution of the experimental data into satellite components.¹⁴ Note that in Table V the two most shifted components of S_2 are reversed in intensity relative to the two most shifted components of S_3 and S_4 .

IV. L_1 COSTER-KRONIG AND FLUORESCENCE YIELDS FOR Sn

In our original calculations of L -shell yields⁴ we used criterion (2) to determine the continuum electron energy for the $L_1-L_3M_{4,5}$ transitions. This proved inaccurate for $Z=47$. For $Z=54$ criteria (2)–(4) do not allow the $L_1L_3M_{4,5}$ transition, and it was not included in the calculations. For $Z=44$ criterion (3) forbids the $L_1-L_3M_{4,5}$ transition while criteria (2) and (4) permit it, the latter by only (+5, +10) eV. For $Z=50$, however, criteria (3) and (4) forbid the $L_1-L_3M_{4,5}$ transition. This leads to new values for Sn, namely, $f_{1,2}=0.154$, $f_{1,3}=0.354$, $\omega_1=0.0388$. The old values, computed assuming $L_1-L_3M_{4,5}$ transitions were allowed, were $f_{1,2}=0.052$, $f_{1,3}=0.784$, and $\omega_1=0.0130$. For Ag the

new (old) value of ω_1 is 0.0329 (0.0102).

V. CONCLUSIONS

Using recent calculations of radiative, Coster-Kronig, and Auger transition rates, and a hypothesis on the origin of x-ray L -series satellite lines, we have computed the silver L -series x-ray spectrum. We have compared the results with experiment, arbitrarily assuming an incident x-ray spectrum. We find that the diagram lines can be reasonably reproduced by allowing the $L_1-L_3M_5$ Coster-Kronig transition but not allowing the $L_1-L_3M_4$ transition. However, for this case the $L_3-M_{4,5}$ satellite is computed to have an intensity four times the measured satellite strength. Since this is a large satellite, we reject the above description. Rather we forbid both $L_1-L_3M_4$ and $L_1-L_3M_5$ transitions and readjust the assumed incident spectrum (initial hole distribution) to bring the total L_1 intensity into agreement with experiment. The intensities of the satellites are then in satisfactory agreement with the measurements.

We have compared the calculated satellite components with those obtained by Parratt from a decomposition of the satellite structure. Agreement is not satisfactory but this may be due to an overestimate of the computed $L-LN_1$ transition rate, to the decomposition of the satellites, or to further Coster-Kronig transitions involving the N_1 hole in the doubly ionized atom.

ACKNOWLEDGMENTS

The author wishes to thank Dr. J. Plimpton and Dr. K. Glibert of Sandia Laboratories for their useful comments.

*Work supported by the U. S. Atomic Energy Commission.

¹F. K. Richtmyer, Rev. Mod. Phys. **9**, 391 (1937).

²R. D. Richtmyer, Phys. Rev. **49**, 1 (1936).

³E. J. McGuire, Phys. Rev. A **5**, 1043 (1972).

⁴E. J. McGuire, Phys. Rev. A **3**, 587 (1971).

⁵E. J. McGuire, Phys. Rev. A **3**, 1801 (1971).

⁶B. Crasemann, M. H. Chen, and V. O. Kostroun, Phys. Rev. A **4**, 2161 (1971).

⁷D. L. Walters and C. P. Bhalla, Phys. Rev. A **3**, 1919 (1971).

⁸L. G. Parratt, Phys. Rev. **54**, 99 (1938).

⁹K. Siegbahn *et al.*, in ESCA, *Atomic, Molecular and*

Solid State Structure Studied by Means of Electron Spectroscopy (Almqvist and Wiksells, Uppsala, Sweden, 1967).

¹⁰A. H. Compton and S. K. Allison, *X-rays in Theory and Experiment* (Van Nostrand, Princeton, N. J., 1935).

¹¹E. J. McGuire, Sandia Research Report No. SC-RR-70-731 (1970) (unpublished).

¹²H. R. Rosner and C. P. Bhalla, Z. Physik **231**, 347 (1970). This published version is a truncated version of the original, and does not contain the individual transition rates.

¹³J. H. Scofield, Phys. Rev. **179**, 9 (1969).

¹⁴L. G. Parratt, Phys. Rev. **50**, 598 (1936).